HYDROGEN FUEL CELL & ENERGY STORAGE
IHFCA IROST

# Modeling of mass transfer in a T-shaped microfluidic fuel cell

**Zahra Sajjadian[1] | Hasan Hassanzadeh[2*]**

[1]PhD student, University of Birjand, Birjand, Iran
[2]Associated Professor, University of Birjand, Birjand, Iran
*Corresponding author, Email: h.hassanzadeh@birjand.ac.ir

**Article Information**

**Article Type:**
Research Article

**Article History:**

Received: 25 March 2023
Received in revised form
22 May 2023
Accepted: 19 June 2023
Published on line 20 June
2023

**Keywords**

Fuel cell
microfluidic
mass transfer
Open-Foam

**Abstract**

The development of microelectronic devices has increased the need for a power supply with high power density for long-term operation. In this article, microfluidic fuel cells (MFCs) are first introduced, and second, due to the significant effect of mass transfer on their performance, mass transfer in these fuel cells is investigated. MFCs have small dimensions and simple geometry, and formic acid and oxygen dissolved in sulfuric acid are usually used as fuel and oxidizers, respectively. The equations of continuity, momentum, and mass transfer have been solved in three dimensions using Open-Foam open-source software to model the MFC and then validated, with the results available in the references. Fick's equation was used to calculate the rate of diffusion, and the Butler-Volmer equation was used to calculate the rates of electrochemical reactions in catalyst layers. Preliminary results indicated that the performance of this fuel cell is greatly limited by poor fuel utilization, which is consistent with the experimental data. The flow is fully developed in this short distance from the inlet ,and in the fully developed area, the ratio $U_{max}/\bar{U}$ is equal 2.1. The mixing zone located at the interface of fuel and oxidizer is in the shape of an hourglass in the cross-section, and as the inlet velocity increases, its thickness decreases along the channel. Also, as the flow moves along the channel, the thickness of the layer with a low concentration near the electrodes increases.

**Cite this article:** Sajjadian, Z., Hassanzadeh, H. (2023). Modeling of mass transfer in a T-shaped microfluidic fuel cell.
DOI:10.22104/HFE.2023.6425.1265

© The Author(s).
Publisher: Iranian Research Organization for Science and Technology(IROST)
DOI: 10.22104/HFE.2023.6425.1265

## 1. Introduction

Due to high energy density and zero emissions, fuel cells are promising energy conversion devices for all application scales, ranging from miniature power supplies to large-scale power plants [1]. Various energy conversion devices have been developed to adapt to different applications, such as electric generators, batteries, and fuel cells.

Fossil-fuel electric generators have low efficiency (20-30%) due to indirect energy conversion; however, as long as they are fed with fuel and oxidizer, they can produce high energy density (~3.2 kWh/kg for a diesel engine with 25% efficiency) [2]. Batteries with direct energy conversion have much higher energy efficiency (80-90%), but their energy density is minimal due to the low storage capacity of reactants (0.3-0.1kWh/kg for lithium-ion batteries). Fuel cells, on the other hand, combine the advantages of electric generators and batteries, resulting in high energy conversion efficiency (40-60%) and high energy density (~19.7 kWh per kilogram for hydrogen fuel, assuming 50% efficiency) [2]. Therefore, this type of energy converter is considered a promising power source for the future. Fuel cells are electrochemical devices that directly convert the chemical energy of the fuel into electrical energy without the limitations of the Carnot cycle [3]. Fuel cells usually divided by the electrolyte they use, the five main categories of fuel cells are: phosphoric acid, molten carbonate, alkaline, solid oxide, and polymer fuel cells. Due to simple kinetics, hydrogen gas is the ideal fuel for all types of fuel cells [4]. In addition to hydrogen, light hydrocarbons can be directly used in high-temperature fuel cells, but it is necessary first to reform the fuel to use these hydrocarbons in low-temperature fuel cells.

Among the different fuel cells, the polymer fuel cell is considered suitable for cars and portable devices due to having solid electrolyte, high efficiency (83% in standard conditions with pure hydrogen) [4], low working temperature (≈80°C), high energy density ($\approx 1.3 kW/L$)[4], low noise (50-60dB) [5] and quick start-up (in seconds). However, it is difficult to manage water and heat in this fuel cell, and it is not possible to make it smaller to any desired amount. Therefore, this type of fuel cell is unsuitable for advancing technology by solving the need for a small energy source; hence, it is necessary to create new fuel cells.

## 2. Microfluidic fuel cell

Advances in miniaturization technology have led to the creation of a new class of power-generating devices for low-power applications. These low-power generating devices are called micro-power generators. Generally, micro-power generators can be classified as (i) chemical-based, including micro-internal combustion engines and micro-turbines; (ii) electrochemical-based, such as batteries and fuel cells; and (iii) direct conversion devices, such as thermoelectric and photovoltaic microstructures. Among these devices, electrochemical power generators are more competitive for various low-power applications such as mobile phones, laptops, etc. [6]

A microfluidic fuel cell is defined as a laminar flow-based fuel cell that follows the electrochemical principles of polymer fuel cells. In addition, a microfluidic fuel cell does not have a membrane, and all the usual polymer fuel cell processes occur in a microchannel. According to Figure 1, this fuel cell has a simple geometry and consists of a microchannel with two electrodes, an anode and a cathode. Electric current is produced by the laminar flow of fuel and oxidizer dissolved in an electrolyte from both sides of the channel and the occurrence of oxidation and reduction reactions on its electrodes. However, with the movement of the fuel and oxidizer flow along the channel and fuel and oxidizer consumption, the concentration in the vicinity of the electrodes decreases. In addition,

the mixing of fuel and dissolved oxidizer at the interface of two streams causes the length of the fuel cell channel to be limited. Unlike polymer fuel cells, this fuel cell does not have a membrane, and the fuel solvent and oxidizing electrolytes are responsible for transferring ions between the two electrodes. This fuel cell does not fall into the usual division of fuel cells, and because it does not have a membrane, it has the following advantages compared to the polymer fuel cell. 1. The absence of a membrane reduces the thickness of the fuel cell and simplifies its design and construction. 2. There are no problems related to water and heat management in the membrane. 3. Fuel and oxidizer flow together in the same channel, so design considerations for fuel and oxidizer supply systems are less complicated. 4. It is easy to make smaller. 5. It uses fuel and oxidizers dissolved in a liquid. The fuel solvent and oxidizing liquid play the electrolyte role, transferring ions between the anode and cathode electrodes.

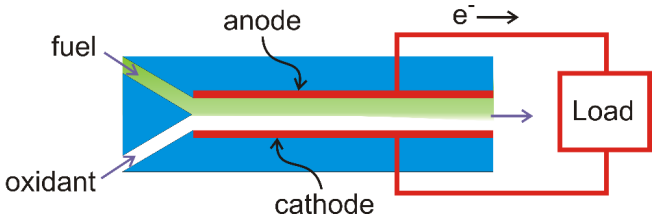


**Fig. 1. Schematic of a microfluidic fuel cell.**

Another advantage of this type of fuel cell is the variety of fuels that it can use. Table 1 lists various fuels that can be used in this fuel cell along with the ideal voltage, kinetic reaction speed, energy per mass unit, and the type of catalyst used, etc. [2]. Among these fuels, formic acid is considered a more suitable fuel for this type of fuel cell, although the formic acid reaction kinetics are somewhat complex and multistep, and not simply the kinetics of the hydrogen reaction.

**Table. 1. Comparison of Different Fuels for MFC Operation.**

| Type of fuel | $\Delta E_0(V)$ | Reaction kinetics | Specific energy (kWh/kg) | Typical catalyst | Fuel cost (USD/kg) | Shortcoming |
|---|---|---|---|---|---|---|
| Vanadium | 1.25 | high | - | Carbon | 14.1 | Toxic |
| Hydrogen | 1.23 | High | 39.4 | Pt | 14 | Storage issue |
| Glycerol | 1.21 | Medium | 5.0 | Pt/Pd | 5.0 | High viscosity |
| Borohydride | 1.64 | Medium | 9.3 | Pt | 10 | Expensive |
| **Formic acid** | **1.45** | **Medium** | **1.73** | **Pd** | **1** | **$CO_2$ bubbling** |
| Ethanol | 1.14 | Medium | 8.0 | Pd/Pt–Ru | 0.42 | Catalyst poison |
| Hydrazine | 1.56 | Medium | 5.47 | Pt | 1 | Toxic |
| $H_2O_2$ | 1.08 | Medium | 0.75 | Pt | 0.8 | $O_2$ bubbling |
| Ammonia | 1.14 | Low | 6.25 | Ni–Cu | 0.5 | $N_2$ bubbling |
| Glucose | 1.09 | Low | 4.43 | Au | 0.5 | Poor efficiency |
| Methanol | 1.21 | Medium | 6.1 | Pt–Ru | 0.4 | Toxic |
| Urea | 1.15 | Low | 3.56 | Ni (alkaline) | 0.22 | $N_2$ bubbling |

Like other fuel cells, this fuel cell has disadvantages that need to be considered. Experimental methods are expensive and time-consuming, so modeling is necessary to increase efficiency and reduce production costs. Various papers on this topic have been published in the field of microfluidic fuel cell modeling, some of which are mentioned here. Chopan et al. [7] experimentally studied the Y-shaped microfluidic fuel cell. The fuel was formic acid dissolved in 0.5M sulfuric acid, and the performance curves, the fuel concentration distribution curve, and the potential in the cross-section along the channel were studied. Bazylak et al. [8] modeled the T-shaped microfluidic fuel cell using computational fluid dynamics. In this modeling, formic acid dissolved in phosphoric acid was used as fuel and oxygen dissolved in sulfuric acid was used

as an oxidizer in a relatively more accurate electrochemical model compared to previous research. The results showed that the geometrical shape has a significant effect on the performance of the fuel cell. In addition, while drawing the distribution of velocity and concentration of fuel and oxidizer in the cross-section of the channel, they suggested different methods to increase fuel consumption. Phirani et al. [9] modeled the mass transfer in a microfluidic fuel cell by assuming a linear velocity distribution in the vicinity of the electrodes. They drew the distribution curve of the fuel and oxidizer concentration in cross-section at a distance of  from the channel's inlet. In addition, by adding an acid flow Sulfuric between two streams of fuel and oxidizer in the microchannel, they presented a method to increase fuel consumption. Sun et al.[10] experimentally investigated the effect of several inlet laminar flows (a laminar flow of sulfuric acid between the fuel and oxidizer flows) on fuel cell performance. Zhu [11] modeled T- and Y-shaped microfluidic fuel cells under the same input conditions and showed that Y-shaped cells perform better than T-type. In addition, in a Y-shaped fuel cell with different inlet angles, the fuel cell with a  inlet performs better. Other types of microfluidic fuel cells have been reviewed in references [6, 12-13].

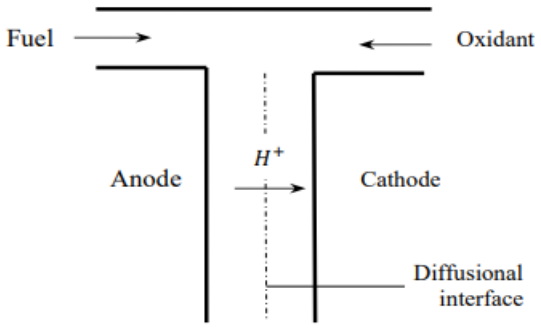


**Fig. 2. Schematic of a T-shape microfluidic fuel cell.**

Since relatively few articles have been published about T-type microfluidic fuel cells, this study investigated mass transfer in T-shaped microfluidic fuel cells. In order to study the mass transfer, the equations of continuity, conservation of momentum, and conservation of mass have been solved in 3D along with the prevailing boundary conditions using Open-Foam open-source software. According to Figure 2, formic acid (HCOOH) and oxidizing oxygen ($O_2$) are dissolved in the background electrolyte, i.e., sulfuric acid ($H_2SO_4$), which flows along the microchannel; with the occurrence of oxidation (1) and reduction (2) reactions on the electrodes, an electric current is produced. The desired channel in this fuel cell has a square cross-section, and the active surfaces of the electrodes are located on both vertical sides of the channel. Oxidation and reduction reactions on the electrodes are as follows [14]:

$$Anode: HCOOH \rightarrow CO_2 + 2H^+ + 2e^- \quad (1)$$

$$Cathode: O_2 + 4H^+ + 4e^- \rightarrow 2H_2O \quad (2)$$

where $E$ and the superscript 0 represent the potential (V) and standard conditions, respectively .Therefore, in standard conditions, the reversible voltage of this fuel cell with formic acid as fuel is equal to 1.43V.

As can be seen, the oxidation and reduction reactions on the electrodes are similar to the oxidation and reduction reactions in the polymer fuel cell, except that a laminar flow of fuel and oxidizer dissolved in a background liquid is used in the fuel cell channel. When the fuel oxidation reaction occurs on the anode electrode, hydrogen ions and electrons are formed. Under the effect of the concentration gradient and electric field gradient, hydrogen ions are transferred from inside the channel, and electrons from the external circuit transfer to the cathode electrode. When the reduction reaction occurs on the cathode electrode, the electric circuit is completed. Table 2 shows some of the physical properties of the fuel and oxidizer passing through the two sides of the channel.

**Table. 2. Fuel and Oxidizer Properties**

| | |
|---|---|
| **Fuel (formic acid)** | $C_F = 2100 mol/m^3$ |
| **Oxidizer (Oxygen)** | $C_O = 0.5 mol/m^3$ |
| **Viscosity[15]** | $\mu = 0.001\ Pa.s$ |
| **Density[15]** | $\rho = 1000 kg/m^3$ |
| **Temperature** | $T = 300k$ |
| **The diffusion coefficient of formic acid [15]** | $D = 5\times10^{-10} m^2/s$ |
| **Oxygen diffusion coefficient [15]** | $D = 2.1\times10^{-10} m^2/s$ |

## 3. Governing equations and boundary conditions

This section presents the governing equations for flow and mass transfer and related boundary conditions.

### 3.1 Governing equations

For low Reynolds numbers, the laminar and incompressible flows in the micro-channel can be described by the Navier-Stokes and continuity equations [14]:

$$\nabla . \vec{u} = 0 \tag{4}$$

$$\rho(\vec{u}.\nabla)\vec{u} = -\nabla p + \mu\nabla^2\vec{u} + F \tag{5}$$

where $\vec{u}$ is the velocity vector of the channel (m/s), ρ is the fluid density of the electrolyte, is the location pressure ($P_a$), and $F$ is the body force ($N/m^3$).
The species equation is given by [8]:

$$\nabla.(\rho\vec{u}\nabla Y_i) = \nabla.\vec{N}_i + S_i \tag{6}$$

where $Y_i = \rho_i/\rho$ is the local mass fraction of species i and $S_i$ is the net rate of production of species i by chemical reaction. The source terms in the mass transfer equation are proportional to $j_a$ and $j_c$, which is expressed by the Butler-Volmer equation. According to this equation, electrochemical reactions in fuel cells take place in the presence of an electric field, and in this case, the activation free energy includes both chemical and electrical quantities[15-16] .

$$J_a = aj_{0,f}\left[\exp\left(\frac{\alpha_a nF\eta}{RT}\right) - \exp\left(\frac{\alpha_c nF\eta}{RT}\right)\right] \tag{7}$$

$$J_c = aj_{0,O}\left[\exp\left(\frac{\alpha_a nF\eta}{RT}\right) - \exp\left(\frac{\alpha_c nF\eta}{RT}\right)\right] \tag{8}$$

In this equation, $\eta$ is activation loss, $j_o$ is exchange current density, $\alpha$ is the charge transfer coefficient, and a is the roughness factor. The values of these parameters are given in Table 3.
For the dilute approximation used in this model, the diffusion flux of species i is given by Fick's law:

$$\vec{N}_i = -\rho D_i \nabla Y_i$$

where $D_i$ is the diffusion coefficient for species i into the mixture.

**Table 3. Kinetics Properties [17]**

| | $\alpha_a$ | $\alpha_c$ | $aj_{0,f}(A/m^3)$ | $aj_{0o}(A/m^3)$ | n |
|---|---|---|---|---|---|
| **Anode** | 0.5 | 0.5 | $3.82\times10^5$ | - | 2 |
| **Cathode** | 0.5 | 0.5 | - | 100 | 4 |

### 3.2 Boundary conditions

The boundary conditions of the velocity at the entrance, at the exit, and on the walls are as follows:

| | |
|---|---|
| **At inlet:** | $u=U_{in}$ |
| **At outlet: fully developed** | $\partial u/\partial y = 0$ |
| **Side, upper, and lower walls: no slip conditions** | $u=0$ |

The boundary conditions of the mass transfer equation at the entrance, the exit, and on the walls are as follows:

| | |
|---|---|
| **At inlet:** | $Y_f = Y_{in,f}, Y_o = Y_{in,0}$ |
| **At outlet: fully developed** | $\partial Y_f / \partial y = 0,\ \partial Y_0 / \partial y = 0$ |
| **Upper and lower walls: non-porous wall** | $\mathcal{N}_f'' \ \& \ \mathcal{N}_o'' = 0$ |

## 4. Solution method and validation

The assumptions used to solve the governing equations are:

- The flow is laminar, incompressible, and steady.
- The fuel cell is isothermal because the dimensions of the fuel cell are small; in addition, the flow velocity is low; therefore, dissipation due to viscosity is negligible [8].
- The physical properties of the electrodes are isotropic and homogeneous.
- Product carbon dioxide is fully dissolved in the solution.
- The fuel solution is diluted in the electrolyte.

Since the geometry is 3D, an open-FOAM numerical code has been used to investigate the flow and concentration distribution [18] . This numerical code is one of the most important and basic open-source software that allows analyzing compressible and incompressible flows, two-phase flow (gas-particle, fluid-fluid), etc. This software is written in C++ and is based on the finite volume method. The geometry and grid of the domain in this software are created using the block mesh tool. Hexagonal cells have been used for the desired geometry. To ensure the numerical results, the test of independence of the solution from the network has been performed using the data from Table 3. For a network with the number of nodes 90*180*90 in the x, y, and z direction, the ratio $U_{max}/\bar{U}$, obtained from the numerical solution, has an approximate error of 1% with reference results [16], showing that this number of nodes is acceptable both in terms of accuracy and calculation time. In order to model the mass transfer, it is necessary to analyze the flow field first. The desired microchannel has a length of 8 mm and a cross-section 1*1mm$^2$ of . To check the correctness of the written program, according to Figure 2, the program was implemented for a rectangular channel with different aspect ratios and a channel ratio of $U_{max}/\bar{U}$ and then compared with the reference results [16]. Also, in Figure 3, the distribution of fuel concentration in the middle plane of the anode electrode and 5 mm from the channel's beginning is compared with the results presented in reference [8], both of which have good accuracy.

**Table 4. Independence of Grid Solution for a Channel with a Square Cross-section**

| Error percentage of the ratio $U_{max}/\bar{U}$ present study with reference [19] | Dimensions of grid division in x, y, z directions |
|---|---|
| 3.49% | 30*150*30 |
| 1.97% | 60*150*60 |
| 1.3% | 75*180*75 |
| 0.97% | 90*180*90 |
| 0.71% | 105*195*105 |

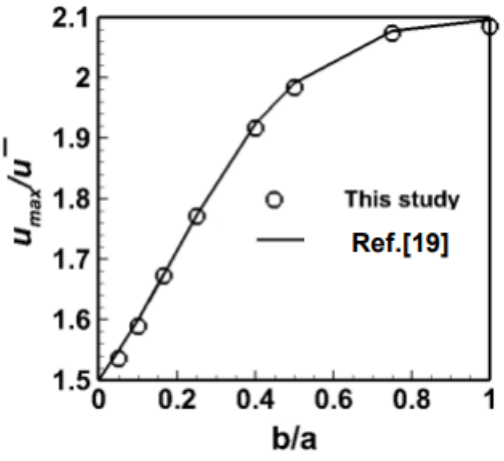


**Fig. 3. Comparison of the curve of changes $u_{max}/\bar{u}$ at different channel aspect ratios with ref. [19].**

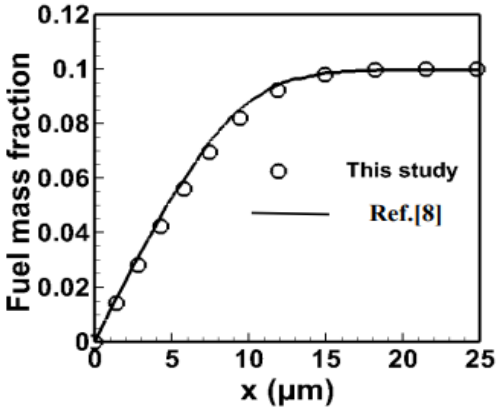


**Fig. 4. Distribution of formic acid concentration perpendicular to the anode electrode (in the middle plane) and at a distance of 5 mm from the beginning of the channel and comparing it with reference results[8]**

## 5. Results and discussions

Figure 5 shows the microfluidic fuel cell and the velocity distribution at y = 6mm from the channel inlet. The velocity distribution of the fuel and oxidizer flow entering the microchannel is uniform and equal to $U_{in}$ = 0.1m/s. Due to the small cross-sectional area of the microchannel, the flow is fully developed in this short distance from the inlet, and in the fully developed area, the ratio $U_{max}/\bar{U}$ in the center line of the channel is 2.1.

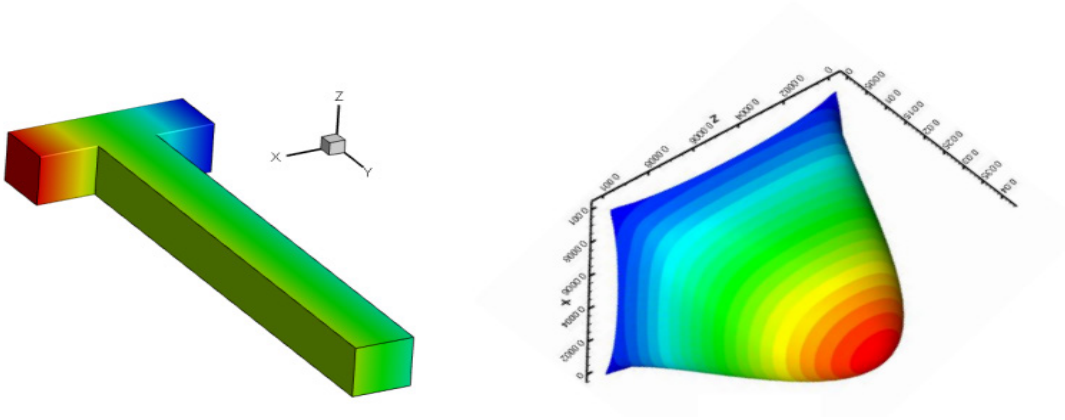

**Fig. 5. Schematic of T-shaped microfluidic fuel cell and velocity distribution in the channel at a distance of y=4mm from the channel entrance.**

Figure 6 shows the distribution of concertation in the cross-section of the channel at y = 1mm from the channel inlet. In this case, only the lateral diffusion of the two fluids at the interface of the two streams is considered, and the reaction on the electrodes is ignored. As can be seen, the diffusion of the two streams of fuel and oxidizer at the top and bottom of the channel is more than the middle area because the longitudinal velocity of the fluid near the top and bottom walls is lower than at the center of the channel, and finally the mixing area is like an hourglass. The thinness of the mixing zone indicates a better separation of fuel and oxidizer in the channel and is desirable. By reducing the speed of the incoming flows, the amount of penetration of fuel and oxidizer into each other increases and the mixing zone becomes wider. The widening of this area can lead to the contact of fuel and oxidizer with the opposite electrodes, which is called a short circuit, and in this case, the efficiency of the fuel cell is greatly reduced.

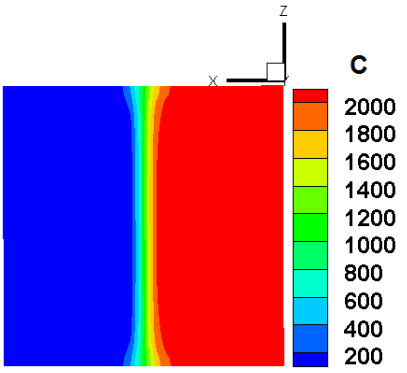


**Fig. 6. Distribution of concentration in the mixing area in the channel cross-section.**

Figure 7 shows the distribution of fuel and oxidizer concentration. The solid and dashed lines indicate the concentration of fuel and oxidizer dissolved in sulfuric acid in the cross-section, respectively. According to the figure, the dissolved fuel was present only on the left side of the channel (anode electrode side), and after a little diffusion on the cathode side, its concentration reached zero. The soluble oxidizer was present only on the cathode side, and after a little diffusion in the middle region, the concentration reached zero on the anode side. Because the reaction on the electrodes is not considered, the distribution of the concentration of the fuel and oxidizer solution is constant on both sides.

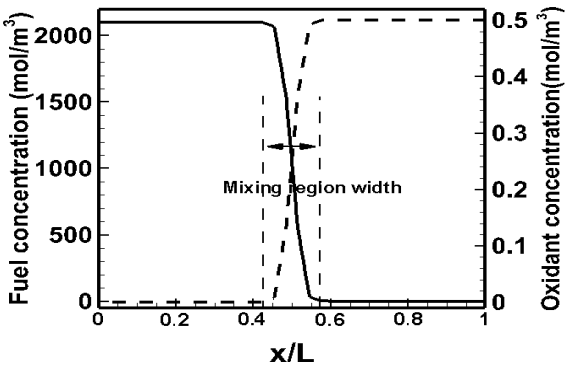


**Fig. 7. Distribution of fuel and oxidizer concentration at the channel cross-section.**

Figure 8 shows the distribution of fuel and oxidizer concentration in the channel cross-section. In addition to diffusion in the interface, electrochemical reactions on the cathode electrode are also considered in this study. As can be seen, a layer with a low concentration has formed in the vicinity of the cathode electrode due to the rapid consumption of reactants near the cathode electrode. The formation of this layer near the electrodes causes the transfer rate of reactants to the reaction sites to decrease, leading to a decrease in the performance of the fuel cell. Therefore, efforts should be made to design the fuel cell channel in such a way that its thickness is as small as possible.

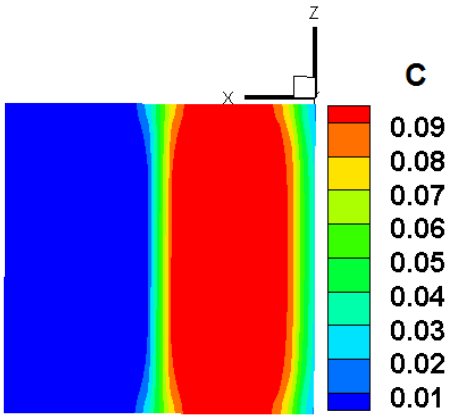


**Fig. 8. Distribution of oxygen concentration on the cross-section of the channel.**

Figure 9 shows the distribution of fuel and oxidizer concentration in the cross-section of the channel at y=1mm from the inlet. As can be seen, the rapid reaction on the surface of the electrodes causes the concentration of reactants near the electrodes to decrease quickly. Gradually, as fuel and oxidizer dissolved in sulfuric acid flows along the channel, the slope of the concentration curve decreases.

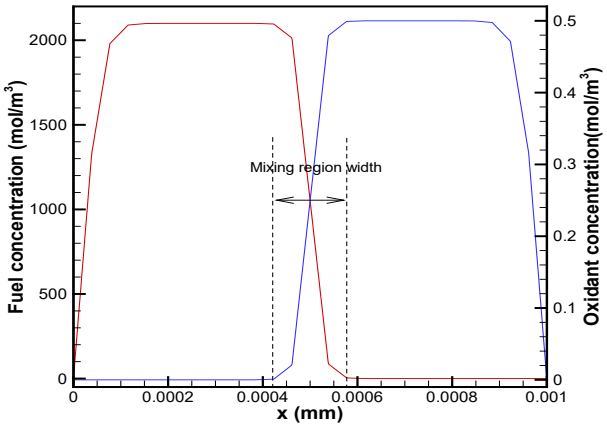


**Fig. 9. Distribution of fuel and oxygen concentration on the cross-section of the channel.**

Figure 10 shows the fuel concentration distribution curve on the anode side at different points along the channel. According to these figures, the fuel concentration on the anode electrode is zero, and in the middle of the channel (x/L=1) is equal to the concentration entering the channel. The concentration was

reduced to zero at the electrode surface, indicating that the reaction kinetics were fast compared to the diffusion in this system. This result agrees with experimental results. Since the fuel cell is diffusion-limited, the geometry of the microchannel plays a dominant role in the efficiency of the cell [7] . As the flow moves along the channel, the fuel concentration gradually decreases due to fuel consumption; therefore, its gradient decreases in the vicinity of the electrode. Low fuel consumption is one of the problems of this type of fuel cell in this simple geometry. In addition, it is difficult to separate the fuel and oxidizer output from the fuel cell.

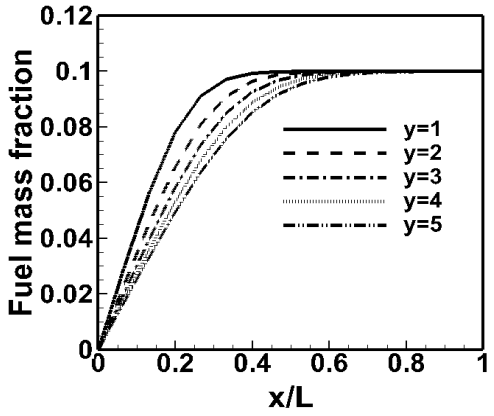


**Fig. 10. Fuel concentration mass fraction curve at different points along the channel.**

## Conclusions

Due to the effect of mass transfer on fuel cell performance and especially on fuel consumption, the issue of mass transfer has been considered in this paper. The study's fuel cell has a three-dimensional channel with a square cross-section, where electrochemical reactions are formed on its sides. The governing equations were solved and validated by Open-FOAM software. The laminar flow of fuel and oxidizer flow parallel to each other along the channel. Due to the same inlet velocity, density, and viscosity for dissolved fuel and oxidizer, the velocity distribution in the cross-section of the channel is completely symmetrical. The diffusion of fuel and oxidizer into each other at the interface and the reduction of concentration in the vicinity of the electrodes were investigated by solving the equations of continuity, momentum, and mass transfer in the channel. The results show that the fuel and oxidizer mixing zone is hourglass-shaped and becomes wider as the distance from the beginning of the channel increases. Also, due to the consumption of fuel and oxidizer, their concentration gradually decreases in the vicinity of the electrodes along the channel, which can reduce the efficiency of the fuel cell. In summary, by changing the geometry, using oxygen in the air instead of dissolved oxygen, and separating the fuel dissolved in sulfuric acid from the free air, the performance of this type of fuel cell can be improved.

## 7. Nomenclature

| | | | |
|---|---|---|---|
| $\vec{u}$ | Velocity vector, m⁄s | T | Temperature, K |
| P | Pressure, pa | $\eta$ | Activation overvoltage (V) |
| C | Concentration, mol⁄m$^3$ | $\alpha$ | Charge transfer coefficient |
| D | Diffusion coefficient, m$^2$⁄s | $j_0$ | Exchange current density (A⁄m$^2$) |

### References

[1] Omid Babaie Rizvan, Serhat Yesilyurt, *Modeling and performance analysis of branched microfluidic fuel cells with high utilization,* Electrochimica Acta, Vol. 318, 2019, p.169-180.

[2] Y. Wang, S. Luo, Holly Y.H. Kwok, W. Pan, Y. Zhang, X. Zhao, Dennis Y.C. Leung, *Microfluidic fuel cells with different types of fuels: A prospective review*, Renewable and Sustainable Energy Reviews 141 (2021) 110806.

[3] H. Hassanzadeh, S. H. Mansouri, *Efficiency of ideal fuel cell and Carnot cycle from a fundamental perspective*, J. of Power and Energy, Vol. 219(2005), p. 245–254.

[4] R. O'Hare, S. W. Cha, W. Colella, F. B. Prinz, Fuel Cell Fundamentals, John Wiley & Sons, 2016.

[5] Matthew M. Mench, *Fuel Cell Engines*, John Wiley & Sons, 2008.

[6] S. A. Mousavi Shaegh, Nam-Trung Nguyen, S. H. Chan, *A review on membraneless laminar flow-based fuel cells*, Int. J. of Hydrogen Energy, Vol.36, 2011, p.5675-5694.

[7] Eric R. Choban, Larry J. Markoski, A. Wieckowski, Paul J.A. Kenis, *Microfluidic fuel cell based on laminar flow*, J. of Power Sources, Vol. 128, 2004, p. 54-60.

[8] A. Bazylak, D. Sinton, N. Djilali, *Improved fuel utilization in microfluidic fuel cells: A computational study,* J. of Power Sources, Vol.143, 2005, p. 57-66.

[9] J. Phirani, S. Basu, *Analyses of fuel utilization in microfluidic fuel cell*, J. of Power Source, Vol. 175, 2008, p. 261–265.

[10] M.H. Sun, G. V. Casquillas, S.S. Guo, J. Shi, H. Ji, Q. Ouyang, Y. Chen, *Characterization of microfluidic fuel cell based on multiple laminar flow,* Microelectronic Engineering, Vol. 84, 2007, p. 1182–1185.

[11] M.N. Nasharudin, S.K. Kamarudin, U.A. Hasran, M.S. Masdar, *Mass transfer and performance of membrane-less micro fuel cell*: *A review*, Inter. J. of Hydrogen Energy, Vol.39, 2014, p. 1039-1055.

[12] Lixin Fan, Zhengkai Tu, Siew Hwa Chan, *Recent development of hydrogen and fuel cell technologies: A review*, Energy Report, Vol. 7, 2021, P. 8421-8446.

[13] B. Zhu, *Microfluidic Fuel Cells – Modeling and Simulation*, MS Thesis, Concordia University, Canada, 2010.

[14] T. Ouyang, F. Zhou , J. Chen , J. Lu , N. Chen, *A novel approach for modelling microfluidic fuel cell coupling vibration*, J. of Power Sources, Vol. 450 ,2020, 227728.

[15] B. Zhang, D. Ye, P. Sui, N. Djilali, X. Zhu, *Computational modeling of air-breathing microfluidic fuel cells with flow-over and flow-through anodes*, J. of Power Sources, Vol. 259, 2014, p. 15-24.

[16] G. Hoogers, Fuel cell technology handbook, 2003, CRC Press.

[17] A. B. Khabbazi, A. J. Richards, M. Hoorfar, *Numerical study of the effect of the channel and electrode geometry on the performance of microfluidic fuel cells*, J. of Power Sources, Vol. 195, 2010, p. 8141-8151.

[18] R. Shah, and A. London, *Thermal boundary conditions and some solutions for laminar duct flow forced convection.* J. of Heat Transfer, Vol. 96, 1974, p. 159-165.

[19] Nima Samkhaniani**,** OpenFOAM9 training via problem-solving [in Persian], 2023.